



CANCER DISCOVERY

Discovery of Biomarkers Predictive of GSI Response in Triple-Negative Breast Cancer and Adenoid Cystic Carcinoma

Alexander Stoeck, Serguei Lejnine, Andrew Truong, et al.

Cancer Discovery 2014;4:1154-1167. Published OnlineFirst August 7, 2014.

Updated version Access the most recent version of this article at:
doi:[10.1158/2159-8290.CD-13-0830](https://doi.org/10.1158/2159-8290.CD-13-0830)

Supplementary Material Access the most recent supplemental material at:
<http://cancerdiscovery.aacrjournals.org/content/suppl/2014/08/08/2159-8290.CD-13-0830.DC1.html>

Cited Articles This article cites by 34 articles, 18 of which you can access for free at:
<http://cancerdiscovery.aacrjournals.org/content/4/10/1154.full.html#ref-list-1>

E-mail alerts [Sign up to receive free email-alerts](#) related to this article or journal.

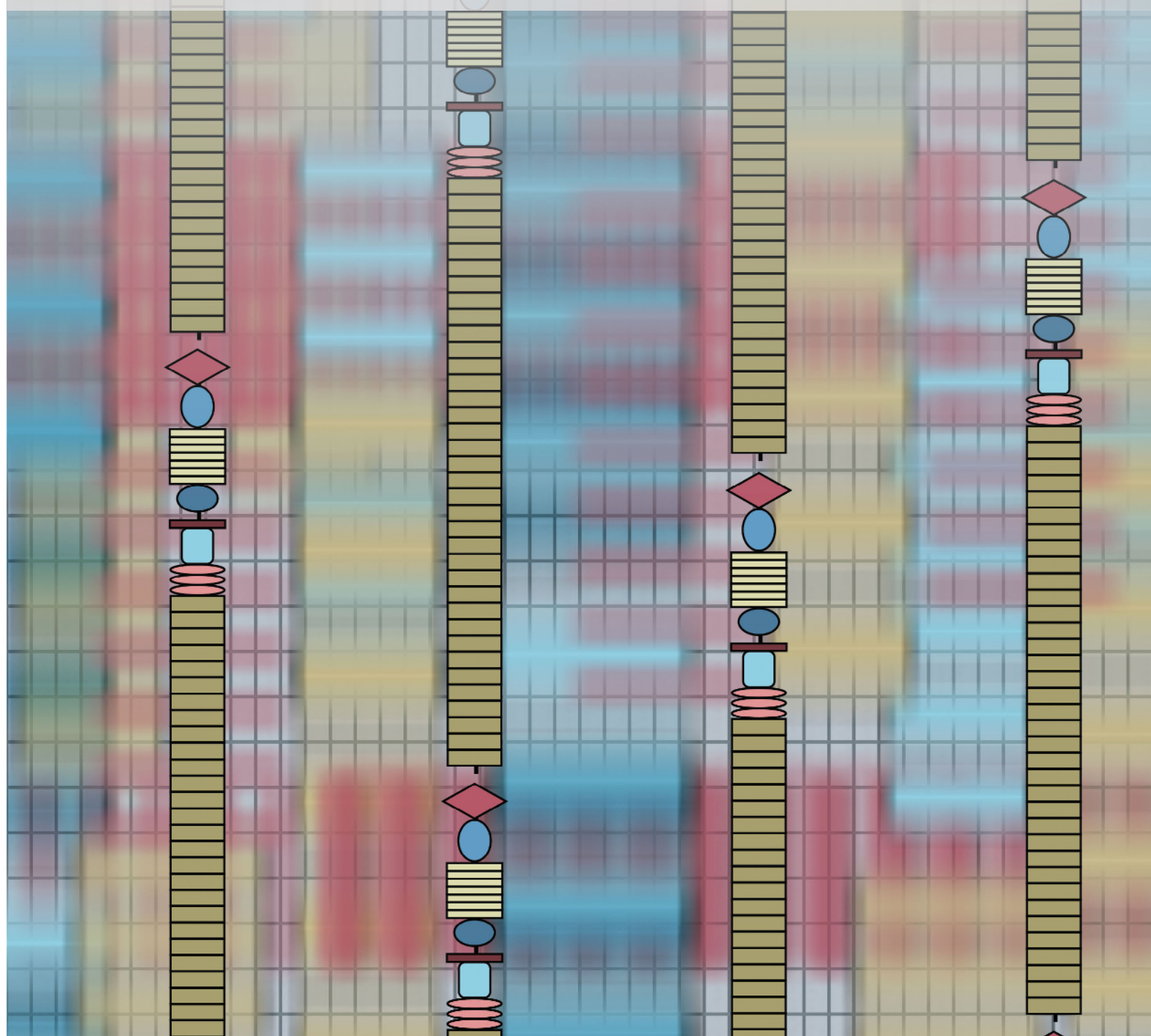
Reprints and Subscriptions To order reprints of this article or to subscribe to the journal, contact the AACR Publications Department at
pubs@aacr.org.

Permissions To request permission to re-use all or part of this article, contact the AACR Publications Department at
permissions@aacr.org.

RESEARCH ARTICLE

Discovery of Biomarkers Predictive of GSI Response in Triple-Negative Breast Cancer and Adenoid Cystic Carcinoma

Alexander Stoeck¹, Serguei Lejnine¹, Andrew Truong¹, Li Pan², Hongfang Wang², Chongzhi Zang³, Jing Yuan¹, Chris Ware¹, John MacLean¹, Philip W. Garrett-Engele¹, Michael Kluk², Jason Laskey¹, Brian B. Haines¹, Christopher Moskaluk⁴, Leigh Zawel¹, Stephen Fawell¹, Gary Gilliland¹, Theresa Zhang¹, Brandon E. Kremer⁵, Birgit Knoechel⁶, Bradley E. Bernstein⁶, Warren S. Pear⁵, X. Shirley Liu³, Jon C. Aster², and Sriram Sathyanarayanan¹



ABSTRACT

Next-generation sequencing was used to identify Notch mutations in a large collection of diverse solid tumors. *NOTCH1* and *NOTCH2* rearrangements leading to constitutive receptor activation were confined to triple-negative breast cancers (TNBC; 6 of 66 tumors). TNBC cell lines with *NOTCH1* rearrangements associated with high levels of activated *NOTCH1* (N1-ICD) were sensitive to the gamma-secretase inhibitor (GSI) MRK-003, both alone and in combination with paclitaxel, *in vitro* and *in vivo*, whereas cell lines with *NOTCH2* rearrangements were resistant to GSI. Immunohistochemical staining of N1-ICD in TNBC xenografts correlated with responsiveness, and expression levels of the direct Notch target gene *HES4* correlated with outcome in patients with TNBC. Activating *NOTCH1* point mutations were also identified in other solid tumors, including adenoid cystic carcinoma (ACC). Notably, ACC primary tumor xenografts with activating *NOTCH1* mutations and high N1-ICD levels were sensitive to GSI, whereas N1-ICD-low tumors without *NOTCH1* mutations were resistant.

SIGNIFICANCE: *NOTCH1* mutations, immunohistochemical staining for activated *NOTCH1*, and *HES4* expression are biomarkers that can be used to identify solid tumors that are likely to respond to GSI-based therapies. *Cancer Discov*; 4(10); 1154–67. ©2014 AACR.

INTRODUCTION

The Notch signaling pathway is an evolutionarily conserved regulator of cell fate, differentiation, and growth. In mammals, Notch signaling is mediated by four Notch receptors (*NOTCH1*–*4*) and at least four functional ligands [Delta-like-1 (DLL1), DLL3, DLL4, JAG1, and JAG2]. Canonical Notch signaling is initiated by ligand binding to the Notch ectodomain. This triggers a series of proteolytic cleavage events, culminating in the release of the Notch intracellular domain (NICD) by gamma-secretase (GS). Upon GS cleavage, NICD translocates to the nucleus, where it forms a Notch transcription complex with the DNA-binding factor CSL (also known as RBPJ) and coactivators of the Mastermind-like (MAML) family (for review, see ref. 1).

Deregulated Notch signaling is oncogenic in specific cell types; for example, it is strongly associated with T-cell acute lymphoblastic leukemia (T-ALL), in which somatic activating mutations in *NOTCH1* are present in >50% of cases (2). Most *NOTCH1* mutations in human T-ALL fall into two classes: (i) in-frame mutations or indels in exons 25 to 28 that disrupt an extracellular juxtamembrane negative regulatory region (NRR), leading to ligand-independent receptor proteolysis and release of the *NOTCH1* intracellular domain (N1-ICD); and (ii) stop codons or frameshift mutations in exon 34 that result in deletion of a C-terminal PEST degron domain, stabilizing N1-ICD. Less commonly in human T-ALL, *NOTCH1* is the target of (7;9) translocations in which the 3' end of *NOTCH1* is fused to promoter/enhancer elements of *TCRB* (3). The rearranged *NOTCH1* alleles in tumors with the t(7;9) drive expression of truncated mRNAs that initiate translation from a conserved methionine lying within the *NOTCH1* transmembrane domain (4).

Oncogenic Notch signaling is also implicated in breast cancer. Recently, RNA-sequencing (RNA-seq) was used to identify abnormal *NOTCH* mRNAs in human breast carcinoma cell lines and primary tumors (5). The aberrant transcripts resulted from cytogenetically silent deletions involving either *NOTCH1* or *NOTCH2*; although several of the rearrangements produce fusion genes, none encode chimeric proteins. Instead, the rearranged *NOTCH1* genes drive expression of truncated mRNAs that initiate translation from the same internal methionine implicated in human T-ALLs with the t(7;9), whereas the rearranged *NOTCH2* genes drive expression of truncated mRNAs that initiate translation from a methionine residue located within the intracellular domain of *NOTCH2*, internal to the GS cleavage site. Because of this distinction, *NOTCH1*-rearranged breast cancers are predicted to be GS inhibitor (GSI) sensitive, whereas *NOTCH2*-rearranged breast cancers are predicted to be GSI resistant.

In addition to its oncogenic roles, genetic evidence suggests that Notch is a tumor suppressor in human squamous cell

¹Merck Research Laboratory, Boston, Massachusetts. ²Department of Pathology, Brigham and Women's Hospital and Harvard Medical School, Boston, Massachusetts. ³Department of Biostatistics and Computational Biology, Dana-Farber Cancer Institute, Boston, Massachusetts. ⁴Department of Medicine and Digestive Health Research Center, University of Virginia, Charlottesville, Virginia. ⁵Department of Pathology, Perelman School of Medicine, University of Pennsylvania, Philadelphia, Pennsylvania. ⁶Department of Pathology and Center for Cancer Research, Massachusetts General Hospital and Harvard Medical School, Boston, Massachusetts.

Note: Supplementary data for this article are available at *Cancer Discovery* Online (<http://cancerdiscovery.aacrjournals.org/>).

A. Stoeck and S. Lejnne contributed equally to this article.

Current address for S. Fawell: AstraZeneca, Waltham, Massachusetts; current address for S. Sathyaranayanan: Jounce Therapeutics Inc., Cambridge, Massachusetts.

Corresponding Authors: Sriram Sathyaranayanan, Jounce Therapeutics, 1030 Massachusetts Avenue, Cambridge, MA 02138. Phone: 508-314-2549; Fax: 617-812-5345; E-mail: ssathy@jountctx.com; Jon C. Aster, jaster@rics.bwh.harvard.edu; and Alexander Stoeck, Alexander.Stoeck@merck.com

doi: 10.1158/2159-8290.CD-13-0830

©2014 American Association for Cancer Research.

carcinoma (SCC). Whole-exome deep sequencing identified likely loss-of-function mutations in at least one Notch signaling component in roughly 15% to 20% of head and neck SCC (6, 7); similarly, at least one putative loss-of-function mutation involving either *NOTCH1* or *NOTCH2* was identified in 19 of 26 primary cutaneous SCC or derived cell lines (8). In addition, one trial of a GSI in patients with Alzheimer disease reportedly led to an increase in skin cancers (9).

Despite concerns about the complications of long-term GSI treatment, preclinical studies in animals and clinical trials in patients with cancer suggest that intermittent treatment with GSIs is well tolerated, and GSIs continue to hold promise as targeted therapy for malignancies in which Notch is an oncogenic driver (9). However, clinical responses to GSIs have been modest, possibly because GSI trials to date have not used biomarkers that predict responsiveness as a criterion for enrollment. To address the need for biomarkers, we first screened large collections of cell lines, primary tumors, and metastases for *NOTCH* gene mutations, reasoning that tumors with gain-of-function mutations are most likely to be sensitive to GSI. Our studies show that triple-negative breast cancers (TNBC) are uniquely enriched among tumors screened for activating *NOTCH1* and *NOTCH2* deletions. Using xenograft models, we demonstrate that the GSI sensitivity of *NOTCH1*-rearranged breast cancer cell lines correlates with N1-ICD levels, and that *NOTCH2*-rearranged tumors are indeed GSI resistant. We also identify other human solid tumors with novel activating point mutations in the *NOTCH1* NRR, including a subset of adenoid cystic carcinoma (ACC) cell lines and primary tumors. Like *NOTCH1*-rearranged breast cancers, xenografted *NOTCH1*-mutated ACCs are GSI sensitive, whereas Notch wild-type (WT) xenografts are not. Finally, we identify *HES4*, a known Notch target gene, as a gene whose expression is correlated with poor clinical outcome in TNBC. Our findings suggest that assessment of *NOTCH* gene mutational status, activated Notch protein levels, and expression levels of particular target genes, such as *HES4* in TNBC, will be useful in selecting patients for GSI trials.

RESULTS

Whole-Exome Sequencing Identifies *NOTCH* Gene Rearrangements in Breast Cancer

To detect *NOTCH* gene rearrangements, we used targeted exome sequencing (TES) data from human cancer cell lines and primary tumors to identify imbalances in exon coverage, which can be used to infer the presence of intragenic rearrangements, particularly deletions. Analysis of TES data from 608 cancer cell lines identified exon imbalances in *NOTCH1* or *NOTCH2* in five cell lines and in one cell line, respectively (Fig. 1A and Supplementary Fig. S1A). Exon imbalances were found only in TNBC lines and stemmed from the deletion of exons encoding the Notch extracellular EGF repeats and NRR. For example, in the MB-157 and MDA-MB157 cell lines, the read coverage of 5' *NOTCH1* exons was markedly lower than that of 3' *NOTCH1* exons (Fig. 1A and 1B). A similar imbalance was observed in the read coverage for 5' and 3' *NOTCH2* exons in the HCC1187 cell line (Supplementary Fig. S1A). Our data are consistent with previously reported *NOTCH* gene

breakpoints in the HCC1187 and HCC2218 cell lines, which were originally suspected based on RNA sequencing data (5), and indicate that exon read imbalances in TES data can be used to identify tumors with *NOTCH1* and *NOTCH2* rearrangements. This capacity was confirmed by the detection of novel *NOTCH1* rearrangements in the MB-157 and MDA-MB-157 cell lines, both of which were derived from the same patient with TNBC. Importantly, a fusion transcript consisting of noncoding RNA derived from *SEC16A*, a gene flanking *NOTCH1* on chromosome 9q34.3, and exons 27 to 34 of *NOTCH1* was identified by sequencing of RNA prepared from the MB-157 cell line (data not shown), consistent with the presence of an interstitial deletion that created a *SEC16A-NOTCH1* fusion gene. Similarly, sequencing of RNA prepared from the HCC1599 cell line confirmed the presence of an aberrant transcript consisting of exon 2 joined out of frame to exon 27 of *NOTCH1*, consistent with the presence of an intragenic deletion involving *NOTCH1*, as described elsewhere (5).

Next, we analyzed whole-exome sequencing data from 66 triple-negative primary breast tumors. We identified *NOTCH1* or *NOTCH2* 5' deletions in six tumors, as indicated by significantly decreased read coverage ($P < 10^{-5}$) in 5' exons as compared with 3' exons (Fig. 1C and 1D; Supplementary Fig. S1B). An excess of transcripts containing 3' *NOTCH* exons was confirmed by RT-qPCR (data not shown). Each of the inferred *NOTCH1* deletions is predicted to create mutated alleles driving the expression of truncated transcripts encoding membrane-tethered *NOTCH1* polypeptides that depend on GS for activity (Supplementary Fig. S1C; refs. 4 and 5). In contrast, as with previously reported *NOTCH2* deletions (5), the rearranged *NOTCH2* alleles are predicted to drive the expression of truncated transcripts encoding constitutively active, GS-independent *NOTCH2* polypeptides (Supplementary Fig. S1C).

TNBC is a molecularly heterogeneous tumor that can be classified on the basis of patterns of gene expression into basal-like, immune, mesenchymal stem cell-like, and luminal androgen receptor subtypes (10). Consistent with previous reports, we observed the highest level of expression of *NOTCH1* mRNA in the basal-like tumors ($P < 0.001$; data not shown). Next, we examined whether the presence of *NOTCH1* or *NOTCH2* rearrangements correlates with a particular subtype of TNBC. Of the 66 tumors analyzed, *NOTCH* gene rearrangements were observed in the basal and luminal androgen receptor subtypes (see Supplementary Table S1), but not in the immune or mesenchymal stem cell-like subtypes.

NOTCH Mutations That Disrupt the NRR Coding Region Are Associated with GSI Sensitivity

To determine the relationship between *NOTCH* gene mutational status and sensitivity to GSI, we evaluated the anti-proliferative activity of MRK-003, a potent and selective GSI (11), in a panel of breast cancer cell lines. T-ALL and mantle cell lymphoma cell lines with mutations that disrupt the *NOTCH1* NRR (2, 4) and TALL1, an additional GSI-sensitive T-ALL line with an activating NRR mutation in *NOTCH3* (J.C. Aster, unpublished data), were included as positive controls. The IC₅₀ for MRK-003 in the TNBC cell lines HCC1599 and MB157 with *NOTCH1* rearrangements

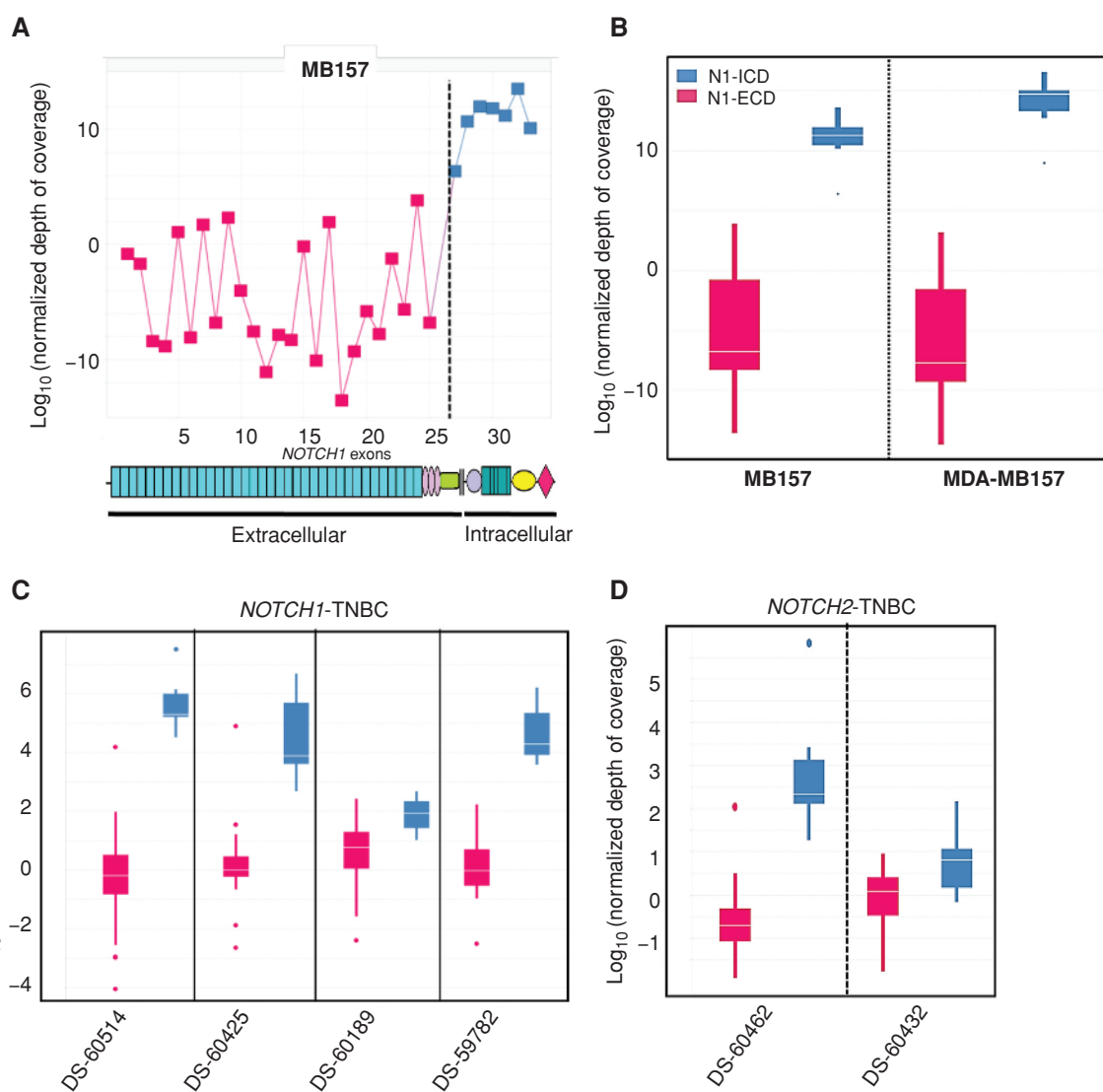


Figure 1. Identification of NOTCH gene rearrangements through analysis of DNA sequencing data. **A**, relative coverage of NOTCH1 exons in the MB157 cell line. Exons 27–34, which encode the NOTCH1 intracellular domain, are shown in blue, whereas exons 1–26, which encode the NOTCH1 extracellular domain, are shown in red. Significant ($P < 10^{-6}$) underrepresentation of reads mapping to exons 1–26 is evident. **B**, boxplots of the read coverage of NOTCH1 exons 1–26 (red) and 27–34 (blue) in cell lines; the boxes span from the 25th to the 75th percentiles, whereas the white line is the median. MB157 and MDA-MB157 show significant ($P < 10^{-5}$) underrepresentation of reads mapping to exons 1–26. The NOTCH1 deletions in these cell lines are heterozygous, as confirmed by RT-PCR (data not shown). N1-ECD, NOTCH1 extracellular domain. **C**, boxplots of the read coverage of NOTCH1 exons 1–26 (red) and 27–34 (blue) in TNBCs. The boxes span from the 25th to the 75th percentiles, whereas the white line is the median. Four of 66 tumors show significant ($P < 10^{-5}$) underrepresentation of read coverage for NOTCH1 exons 1–26. **D**, the same analysis as in **C** for NOTCH2. Two of 66 tumors show significant ($P < 10^{-5}$) underrepresentation of the read coverage for exons 1–26.

was $<1 \mu\text{mol/L}$, similar to the sensitivity of lymphoid cell lines with NOTCH1 or NOTCH3 point mutations or gene rearrangements that disrupt the NRR coding region (Fig. 2A and Supplementary Fig. S2A). In contrast, the HER2⁺ breast cancer cell line HCC2218, which also harbors a SEC16A-NOTCH1 fusion gene (5), demonstrated intermediate sensitivity (Fig. 2A and Supplementary Fig. S2A). As a group, breast cancer cell lines with NOTCH gene rearrangements that disrupt the NRR coding region were significantly more sensitive to MRK-003 than cell lines with WT NOTCH alleles, with two exceptions, the HCC1187 and MDA-MB-157 cell

lines. HCC1187, a breast cancer cell line harboring a SEC22-NOTCH2 fusion gene (5), was predicted to be GSI resistant because the translation start site in aberrant NOTCH2 transcripts is internal to the site of GS cleavage (Supplementary Fig. S1C). In contrast, the resistance of the cell line MDA-MB-157 (Supplementary Fig. S2A) was unexpected, as this line has a deletion that disrupts the NOTCH1 NRR coding region. We also noted that the mantle cell lymphoma cell lines (Mino and MT3), which harbor NOTCH1 mutations leading to deletion of the C-terminal PEST domain, were also resistant to MRK-003. Thus, GSI sensitivity is confined

RESEARCH ARTICLE

Stoeck et al.

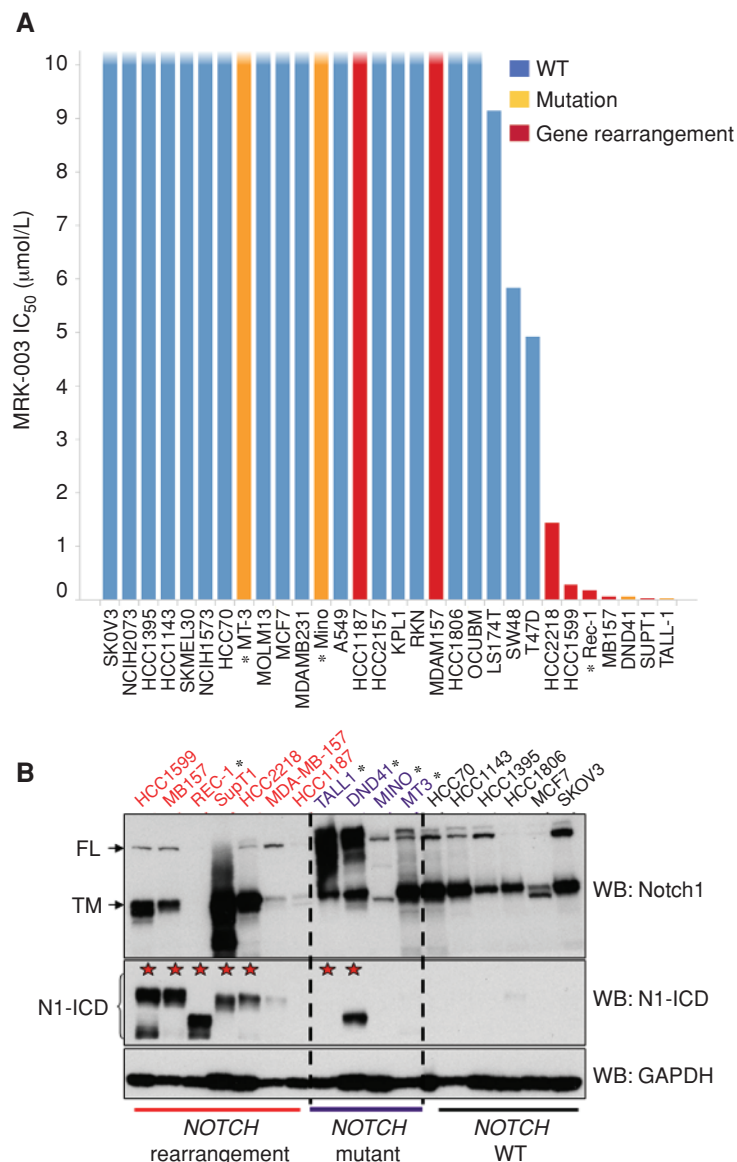


Figure 2. Notch mutational status determines pathway activity and sensitivity to MRK-003 in cancer cell lines. **A**, a panel of cancer cell lines was treated with increasing concentrations of MRK-003 for 72 hours, and the IC₅₀ was determined for cell proliferation as described in Methods. Cell lines harboring NOTCH1 rearrangements (red) or mutations (orange) showed sensitivity to the GSI MRK-003. * MT3, Mino, PEST mutations; REC-1, DND41: dual ectodomain and PEST mutations; TALL-1, high N3-ICD levels. **B**, Western blot analysis on selected cell lines harboring NOTCH1 rearrangements (red), point mutations (purple), or WT (black) alleles. Blots were stained with antibodies specific for the intracellular domain of NOTCH1, which recognize the full-length NOTCH1 polypeptide (N1-FL) and the furin-cleaved N1-TM subunit, or an antibody specific for GS cleaved, activated NOTCH1 (N1-ICD). Equal loading was confirmed by staining with an antibody against GAPDH. Red stars represent cell lines sensitive to MRK-003 treatment.

to cell lines with mutations that disrupt the NRR, but this association is not absolute.

MRK-003 Sensitivity Correlates with NICD Levels

To assess the relationship between NOTCH1 mutational status, Notch signal strength, and GSI sensitivity, we evaluated N1-ICD protein levels. We observed high levels of N1-ICD in most cell lines with NOTCH1 gene rearrangements or mutations involving the NRR (Fig. 2B). Of interest, the exception to this rule is the GSI-resistant MDA-MB157 cell line, which had low levels of N1-ICD despite the presence of a NOTCH1 rearrangement (Fig. 2B). As expected, N1-ICD levels were low or absent in GSI-resistant NOTCH1 WT cell lines, as well as in GSI-resistant mantle cell lymphoma lines (MT3 and Mino), which harbor only PEST domain mutations (Fig. 2B). This is consistent with studies showing that although PEST domain mutations stabilize NICD, they have no effect on NICD levels in the absence of NRR mutations or exposure to ligands (2). As a consequence, N1-ICD protein

level was more highly correlated with GSI sensitivity than NOTCH gene mutational status (Supplementary Fig. S2B and S2C).

We also compared the protein levels of all four Notch receptors in the breast cell line panel ($n = 8$; Supplementary Fig. S2D) using antibodies that recognize full-length Notch receptors and their furin-cleaved transmembrane subunits. We observed variable levels of all four receptors, expression of which did not correlate with sensitivity to MRK-003. For example, high NOTCH1 polypeptide levels were observed in both GSI-sensitive HCC1599 cells and GSI-resistant HCC70 and SKBR3 cells. Similarly, NOTCH2–4 polypeptide levels did not correlate with sensitivity to MRK-003 in this breast cancer cell line panel. These results suggest that N1-ICD level is more highly associated with sensitivity to MRK-003 treatment than expression of Notch receptors *per se*, with the important caveat that reagents to identify other forms of activated Notch receptors (N2-4-ICD) are not yet available.

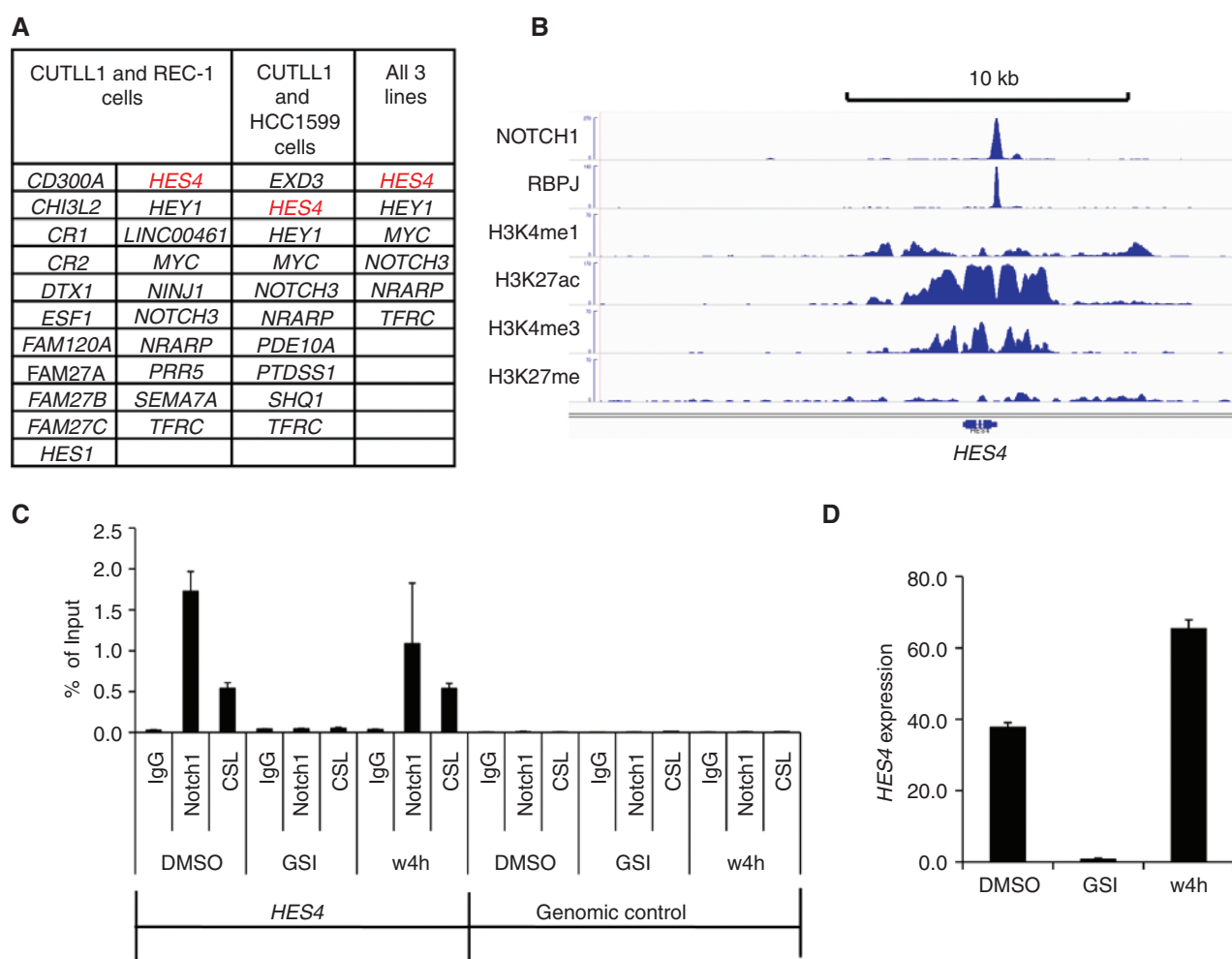


Figure 3. *HES4* is a direct Notch1 target gene in diverse Notch-addicted cancer cell lines. **A**, summary of overlapping direct Notch1 target genes in the T-ALL cell line CUTLL1, the mantle cell lymphoma cell line REC-1, and the TNBC cell line HCC1599. **B**, chromatin landscapes near *HES4* in CUTLL1 cells. A GSI-sensitive RBPJ-NOTCH1 binding site is present in the *HES4* promoter. **C**, NOTCH1-RBPJ complexes associate with the *HES4* promoter site in REC-1 cells. Local ChIP for NOTCH1 and RBPJ was performed under steady-state conditions (DMSO), in cells treated with the GSI compound E (1 μmol/L) for 72 hours (the Notch-off state), and in cells treated for 72 hours with GSI followed by 4 hours of recovery following GSI washout (w4h). **D**, *HES4* expression in HCC1599 cells is Notch dependent. RT-PCR with *HES4*-specific primers was performed under steady-state conditions (DMSO), in cells treated with the GSI compound E (1 μmol/L) for 72 hours, and in cells treated for 72 hours with GSI followed by 4 hours of recovery following GSI washout (w4h).

HES4 Expression Correlates with Notch Activation in Multiple Tumor Types and with Outcome in Triple-Negative Breast Cancer

Although NICD would appear to be a promising biomarker, because sensitive and specific antibodies only exist for detection of N1-ICD, additional markers of Notch activation in diverse cellular lineages are needed. To identify Notch target genes in Notch-addicted cancer cell lines in an unbiased fashion, we performed RNA-seq on CUTLL1 T-ALL cells, REC-1 mantle cell lymphoma cells, and HCC1599 cells (Gene Bank accession number GSE59810), all of which have mutations that disrupt the NOTCH1 NRR. RNA-seq was performed in the Notch-off, GSI-treated state, and 4 hours following washout of GSI, a strategy that rapidly generates N1-ICD and upregulates NOTCH1 target genes in a temporally controlled fashion. Notably, although >80 genes were upregulated upon GSI washout in each cell line (FDR < 0.05), only 6 target genes

were common to all three cell lines—HEY1, MYC, NOTCH3, TFRC, NRARP, and *HES4* (Fig. 3A). Chromatin immunoprecipitation sequencing (ChIP-Seq) analysis of CUTLL1 cells (12) showed that NOTCH1 and RBPJ bind to a site in the *HES4* proximal promoter on chromosome 1 (Fig. 3B). To confirm that this site is highly dynamic, a feature that characterizes functional RBPJ-NOTCH1 binding sites (13), we performed local ChIP for RBPJ and NOTCH1 in REC-1 cells. This showed that GSI depleted NOTCH1 from the *HES4* promoter, and that GSI washout resulted in rapid reloading of NOTCH1 onto this site (Fig. 3C). Finally, we confirmed that GSI markedly inhibited *HES4* expression in HCC1599 cells, and that GSI washout rapidly restored expression (Fig. 3D).

To further study the relationship between activating NOTCH1 mutations and gene expression, we carried out Affymetrix-based microarray analysis in the panel of 608 cell lines (Gene Bank accession number GSE59242) screened previously for NOTCH gene mutations using TES. We observed

that high *HES4* expression was significantly correlated (FDR <0.05) with the presence of activating mutations involving *NOTCH* genes in several cancer cell lines (Supplementary Fig. S3 and Supplementary Table S2). We next compared expression levels of various Notch target genes among primary TNBCs, and noted that *HES4* was the gene whose expression was most strongly correlated with *NOTCH* gene rearrangements in TNBC (Supplementary Table S3). High *HES4* expression was also associated with poor patient outcome in TNBC (log-rank $P < 0.0001$), as patients with metastatic disease in the *HES4*-high group had a median survival of 0.89 years [$n = 21$; 95% confidence interval (CI), 0.31], whereas patients with metastatic disease in the *HES4*-low group had a median survival of 2.97 years ($n = 139$; 95% CI, 2.18; Supplementary Fig. S4). Similarly, in patients without measurable metastatic disease, high *HES4* expression in primary tumors also predicted a poor prognosis (Supplementary Fig. S4). These results suggest that *HES4* expression levels (and by extension, activated Notch levels) may be a useful prognostic biomarker in patients with TNBC.

Notch Inhibition by GSI Is Associated with Induction of Senescence and Apoptosis and Downregulation of MYC in Tumor Models with NOTCH Gene Rearrangements

To investigate how GSI affects cell growth in *NOTCH* gene-rearranged breast cancer models, we evaluated the effect of GSI treatment on molecular pathways regulated by Notch. MRK-003 treatment resulted in a dose-dependent decrease in the levels of activated Notch as measured by N1-ICD in the *NOTCH1*-rearranged TNBC cell lines MB-157 and HCC1599 (Fig. 4A). NOTCH1 inhibition was accompanied by decreases in MYC protein and RB phosphorylation and increases in the level of the cyclin-dependent kinase (CDK) inhibitor p21 (Fig. 4A). In addition, compensatory activation of the MAPK-PI3K pathway was observed, as indicated by GSI dose-dependent increases in phosphorylation of ERK and PRAS40, an AKT substrate (Fig. 4A). These results suggest the existence of a compensatory feedback loop between Notch and the PI3K-MAPK signaling pathways in Notch-dependent breast cancer cell lines. In contrast, MRK-003 treatment did not significantly affect any of these signaling events in the Notch WT cell line HCC1143.

To investigate possible synergistic antitumor effects of Notch and PI3K-MAPK pathway coinhibition, we performed cell proliferation assays in the presence of MRK-003 and a selective ERK inhibitor (SCH772984; ref. 14). MRK-003 treatment produced dose-dependent growth inhibition of both MB-157 and HCC1599, but ERK inhibition failed to potentiate the effect of MRK-003 (see Supplementary Fig. S5). Although these *in vitro* studies were negative, given the evidence of cross-talk between Notch and MAPK-PI3K signaling in breast cancer cells shown here and in other tumor cell types such as T-ALL cells (15), further evaluation of this combination in breast cancer may be warranted.

Next, we evaluated the effects of GSI treatment of *NOTCH* gene-rearranged breast cancer cell lines on cell-cycle progression and apoptosis. MRK-003 treatment resulted in a G₁ cell-cycle arrest and the appearance of a sub-G₁ population, suggestive of apoptotic cell death, in MB-157 cells (Fig. 4B).

Similar effects were also observed in the HCC1599 cells (data not shown). Furthermore, MRK-003 treatment resulted in a dose-dependent increase in cleaved PARP in HCC1599 cells (Fig. 4C), whereas no significant change in cleaved PARP was observed in the *NOTCH2*-rearranged, GSI-resistant cell line HCC1187 (5). In the *NOTCH1*-rearranged MB-157 cell line, MRK-003 produced only a modest increase in apoptosis (data not shown), suggesting that GSI-mediated growth inhibition may stem from a different mechanism in this line. Consistent with this idea, we noted that prolonged MRK-003 treatment of MB-157 cells resulted in the induction of cellular senescence, as measured by β-galactosidase activity (Fig. 4D). Furthermore, robust GSI-mediated upregulation of p21 and downregulation of MYC, events implicated in induction of cellular senescence (16), were also observed in MB-157 cells (Fig. 4A).

The Notch pathway has also been suggested to be important in the maintenance of stem-like cells with tumor-initiating activity (17) and to promote the growth of breast epithelial cells as mammospheres in culture, a phenotype linked to stem-like properties (5, 18). We evaluated the effect of MRK-003 treatment on stem-like cells using the markers CD44/CD24 and aldehyde dehydrogenase (ALDH). When cultured in stem cell media, MB-157 cells contain a subpopulation (~8%) of CD44⁺/CD24^{low} stem-like cells that is depleted by MRK-003 treatment (Supplementary Fig. S6A). Similarly, MRK-003 treatment of MB-157 cells also suppressed the ALDH⁺ cell population (Supplementary Fig. S6B), another marker of cells with stem-like properties. Unlike the effects of MRK-003 on growth, which were restricted to breast cancer lines with *NOTCH1* rearrangements, MRK-003 treatment also suppressed the ALDH⁺ cell population in NCIH226 and MFM223 cells (Supplementary Fig. S6C), which have WT *NOTCH* alleles. Thus, *NOTCH* gene rearrangements do not correlate with the effect of MRK-003 on breast cancer stem-like cells, possibly because the dose of Notch that is required to maintain stem-like cells is substantially lower than that required to drive cell growth. Taken together, Notch signaling in *NOTCH1*-rearranged TNBC cell lines appears to support cell growth through multiple mechanisms, including promotion of cell-cycle progression, decreased apoptosis, and cellular senescence, and increasing the fraction of stem-like cells.

In Vivo Efficacy of GSI Therapy in TNBC Models with NOTCH Gene Rearrangements

We next evaluated the effect of MRK-003 therapy on the growth of breast cancer xenograft models with *NOTCH1* or *NOTCH2* rearrangements (Table 1). MDA-MB-231, a TNBC cell line with WT *NOTCH* alleles, was used as a control model. To identify new primary tumor-derived xenograft models with *NOTCH1* rearrangements, we used RT-PCR to screen for previously described *NOTCH1* rearrangements (5). Of the 21 primary human tumor-derived TNBC xenograft models screened, two models, HBCx8 and HBCx14, yielded RT-PCR products consistent with the presence of *NOTCH1* rearrangements. In HBCx8 cells, we observed a SEC16A-NOTCH1 fusion transcript identical to the previously described rearrangements (data not shown). In HBCx14 cells, we were unable to detect RT-PCR products containing both exons 26 and 28 of *NOTCH1* (data not shown); although this was consistent with the presence of a *NOTCH1* rearrangement,

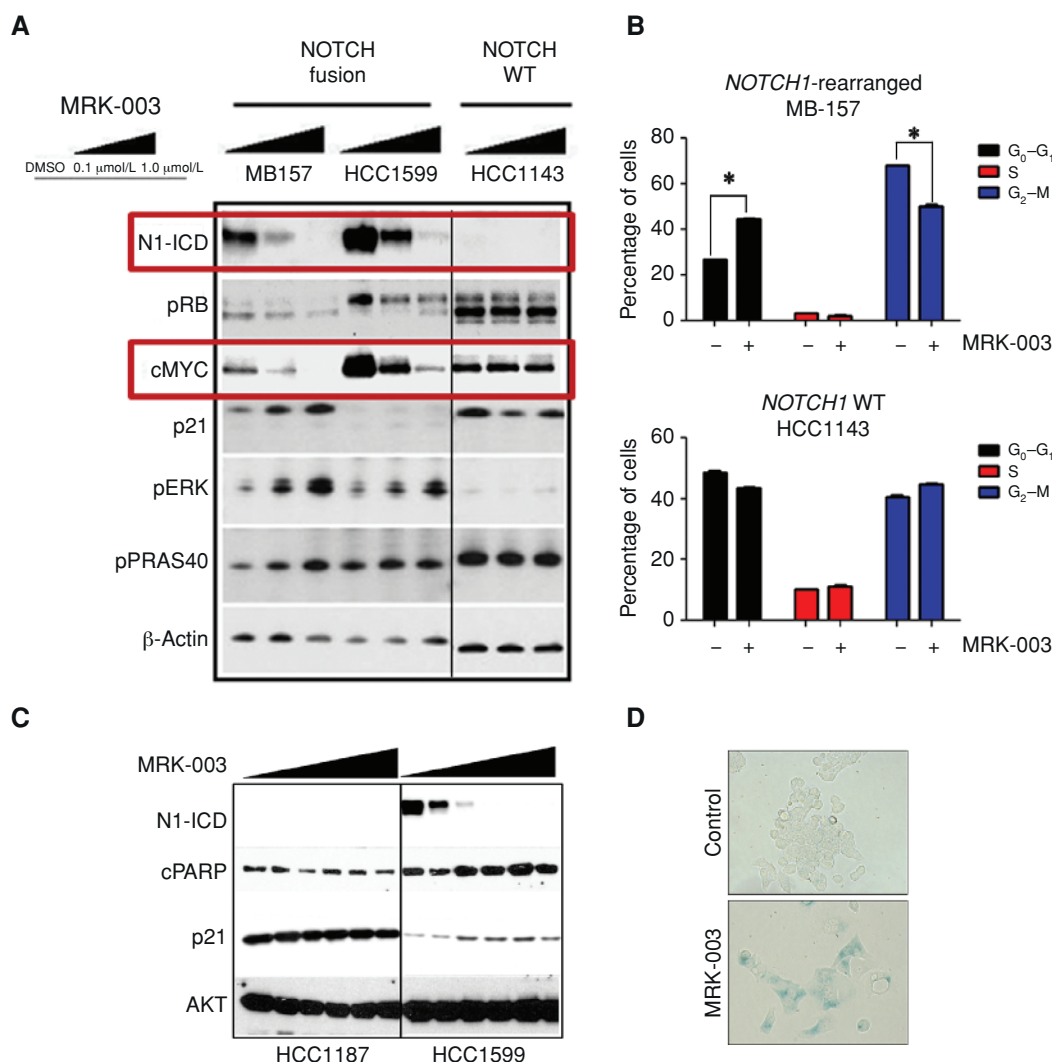


Figure 4. MRK-003 induces cell-cycle arrest, apoptosis, and senescence in cancer cell lines harboring NOTCH1 gene rearrangements. **A**, Western blot analysis on lysates prepared from cell lines with or without NOTCH1 gene rearrangement following treatment with MRK-003 or vehicle (DMSO) for 24 hours. Primary antibodies used were specific for activated NOTCH1 (N1-ICD), pRB, MYC, p21, pERK, pPRAS40, and β-actin (loading control). **B**, cell-cycle analysis performed following treatment of NOTCH1-rearranged MB157 cells and HCC1143 cells with WT NOTCH1 alleles with 1 μmol/L MRK-003 for 72 hours. *, p < 0.05. **C**, HCC1599 cells harboring a NOTCH1 rearrangement and HCC1187 cells harboring a NOTCH2 rearrangement were treated with increasing concentrations of MRK-003 for 24 hours. Western blots were stained with antibodies specific for N1-ICD, cleaved PARP (c-PARP), p21, and total AKT (loading control). **D**, induction of senescence. β-Galactosidase staining was performed after once-weekly treatment of MB157 cells with 1 μmol/L MRK-003 or DMSO (vehicle) for 4 weeks. More than 95% of cells treated with MRK-003 were positive for β-galactosidase, compared with 1% of the cells exposed to DMSO.

Table 1. Summary of antitumor activity of MRK-003 alone or in combination with paclitaxel in TNBC xenograft models

Cell line	NOTCH1 status	MRK-003 (300 mpk)	Paclitaxel (15 mpk)	MRK-003 + paclitaxel	IHC score
HCC1599	Rearranged	90% (TGI)	1% (TGI)	98% (TGI)	+++
MB-157	Rearranged	22% (Reg)	73% (TGI)	72% (Reg)	++
HBCx14	Rearranged	19% (TGI)	-19 (TGI)	67% (TGI)	+
HBCx8	Rearranged	46% (TGI)	22% (TGI)	75% (TGI)	+
HCC1187	WT ^a	-34% (TGI)	48% (TGI)	76% (TGI)	Neg
MDA-MB-231	WT	27% (TGI)	74% (TGI)	86% (TGI)	Neg

IHC score: N1-ICD staining intensity.
Abbreviations: mpk, mg per kg; Reg, tumor regression; TGI, tumor growth inhibition.
^aNOTCH2 translocation resulting in loss of the GSI cleavage site.

we were unable to identify fusion junctions corresponding to previously described *NOTCH1* rearrangements, suggesting that this line harbors a novel *NOTCH1* rearrangement.

To determine whether *NOTCH1* rearrangements correlate with *NOTCH1* activation *in vivo*, we evaluated N1-ICD levels using a sensitive immunohistochemical staining method that is specific for N1-ICD (19). High levels of N1-ICD staining were detected in the HCC1599 and MB-157 models (Supplementary Fig. S7A), a result that correlated well with the results of Western blotting for N1-ICD (Supplementary Fig. S7B). However, HBCx14 had lower levels of N1-ICD staining, and even less staining for N1-ICD levels was seen in the HBCx8 model, despite the presence of a *SEC16A-NOTCH1* fusion gene. As expected, models with WT *NOTCH1* alleles were negative for N1-ICD staining. Next, we evaluated the sensitivity of these xenograft models to GSI treatment, given either alone or in combination with paclitaxel *in vivo*. We noted that sensitivity to MRK-003, alone or in combination with paclitaxel, was associated with N1-ICD levels; these results are summarized in Table 1. For example, MRK-003 treatment produced dose-dependent growth cessation or regression of HCC1599 and MB-157 xenografts (Fig. 5A and Table 1), but had only modest antitumor activity in the MDA-MB-231 xenograft model with WT *NOTCH* genes (Supplementary Fig. S7C and Table 1). Although previous studies have demonstrated significant antitumor activity with MRK-003 in the MDA-MB-231 mode, we would like to note that the dosing scheme used in these studies was not identical to that of our study (20). In this study, we used a clinically tolerated dosing schedule (once a week dosing). Similarly, the HCC1187 xenograft model with a *SEC16-NOTCH2* fusion gene encoding NOTCH2 polypeptides that do not require GS cleavage for activation was resistant to GSI therapy (Fig. 5B). Monotherapy with MRK-003 had modest antitumor activity in the primary human tumor-derived xenografts HBCx8 and HBCx14 (Fig. 5 and Table 1), which have low N1-ICD levels (Supplementary Fig. S7A and S7B). These results indicate that N1-ICD levels can be substantially different in tumors with similar *NOTCH1* rearrangements, and suggest that N1-ICD levels are more highly correlated with GSI responsiveness than *NOTCH* mutational status *per se*.

To further evaluate the association of the antitumor activity of MRK-003 with Notch pathway inhibition, we studied the effect of MRK-003 on Notch target gene expression in the HCC1599 xenograft model. Dose-dependent inhibition of multiple direct or indirect Notch target genes was observed in MRK-003-treated tumors (Fig. 5C), which also showed depletion of N1-ICD, as judged by immunohistochemistry (Fig. 5D). These data confirm that inhibition of the Notch pathway is correlated with the antitumor activity of MRK-003.

Multiple Notch targets may contribute to the antitumor activity of MRK-003 *in vivo*, but one that may be of special importance is MYC, which, as previously noted (Fig. 3), is one of the few common target genes across multiple types of Notch-“addicted” cancer cells *in vitro*. Treatment of HCC1599 xenografts with MRK-003 downregulated MYC protein levels, as judged by Western blotting and immunohistochemistry (Supplementary Fig. S7D), an alteration that was accompanied by decreases in cyclin E, which is involved in G₁-S phase progression. Regulation of MYC by Notch has been docu-

mented in T-ALL (21–24) and in murine models of breast cancer (25), and our results suggest that targeting of the Notch-MYC signaling axis also underlies the responsiveness of human breast cancer models to MRK-003.

Combination Therapy with GSI and Paclitaxel in Breast Cancer Models

We next evaluated the effect of combination therapy with GSI and paclitaxel, an agent that is frequently used to treat TNBC. Modest antitumor activity was observed with single-agent paclitaxel in the *NOTCH1*-rearranged breast tumor models. Although GSI monotherapy resulted in significant growth inhibition of HCC1599 or MB-157 cells, combination therapy with MRK-003 and paclitaxel significantly potentiated antitumor activity in both models and resulted in tumor regression in the MB-157 xenograft model (Fig. 5E). In the primary human tumor-derived xenograft models with *NOTCH1* rearrangements, HBCx8 and HBCx14, monotherapy with MRK-003 or paclitaxel was ineffective in blocking tumor growth, but combination treatment showed significant antitumor activity (Fig. 5F and Table 1), whereas no potentiation was observed in a model with WT *NOTCH* alleles. These results suggest that GSI-paclitaxel combination therapy may be effective in treatment of *NOTCH1*-rearranged tumors.

Characterization of Novel *NOTCH1* NRR Mutations

TES of more than 4,000 tumors identified several novel *NOTCH* gene mutations. As described previously, Notch mutations can be activating or inactivating, depending on the location and nature of the substitution (26). To assess possible gain-of-function mutations, we focused on *NOTCH1* mutations affecting the NRR region or the PEST domain (Supplementary Table S4). *NOTCH* gene mutations in the NRR region and PEST domain were restricted to a small fraction of tumors (<5%), and most of these mutations mapped to the core of the NRR (Fig. 6A), a region frequently involved by gain-of-function *NOTCH1* mutations in human T-ALL (2). Tumor types in which recurrent Notch NRR and PEST domain mutations were identified are summarized in Supplementary Table S5. Of note, NRR or PEST domain mutations were identified in five of 105 TNBCs (Supplementary Table S5). NRR mutations were also observed in one of three ACCs, in line with recent sequencing studies that identified possible Notch gain-of-function mutations in a subset of ACCs (27). To test whether these newly identified *NOTCH1* mutations affect function, they were scored for their ability to activate a Notch-responsive luciferase reporter gene (Fig. 6B). All mutations within the *NOTCH1* NRR caused significant increases in MRK-003-sensitive luciferase activity, with amino acid substitutions at positions 1680, 1570, 1575, and 1683 having the greatest effect. In contrast, in accordance with previous studies, mutations in the PEST domain did not significantly increase luciferase reporter activity in the absence of ligand-mediated stimulation (data not shown).

To investigate the possible role of Notch in ACC, we sequenced *NOTCH1* in six primary tumor-derived xenograft models (see Supplementary Table S6). This led to the identification of *NOTCH1* mutations in two ACC models, both of which were tested for GSI sensitivity. MRK-003 treatment

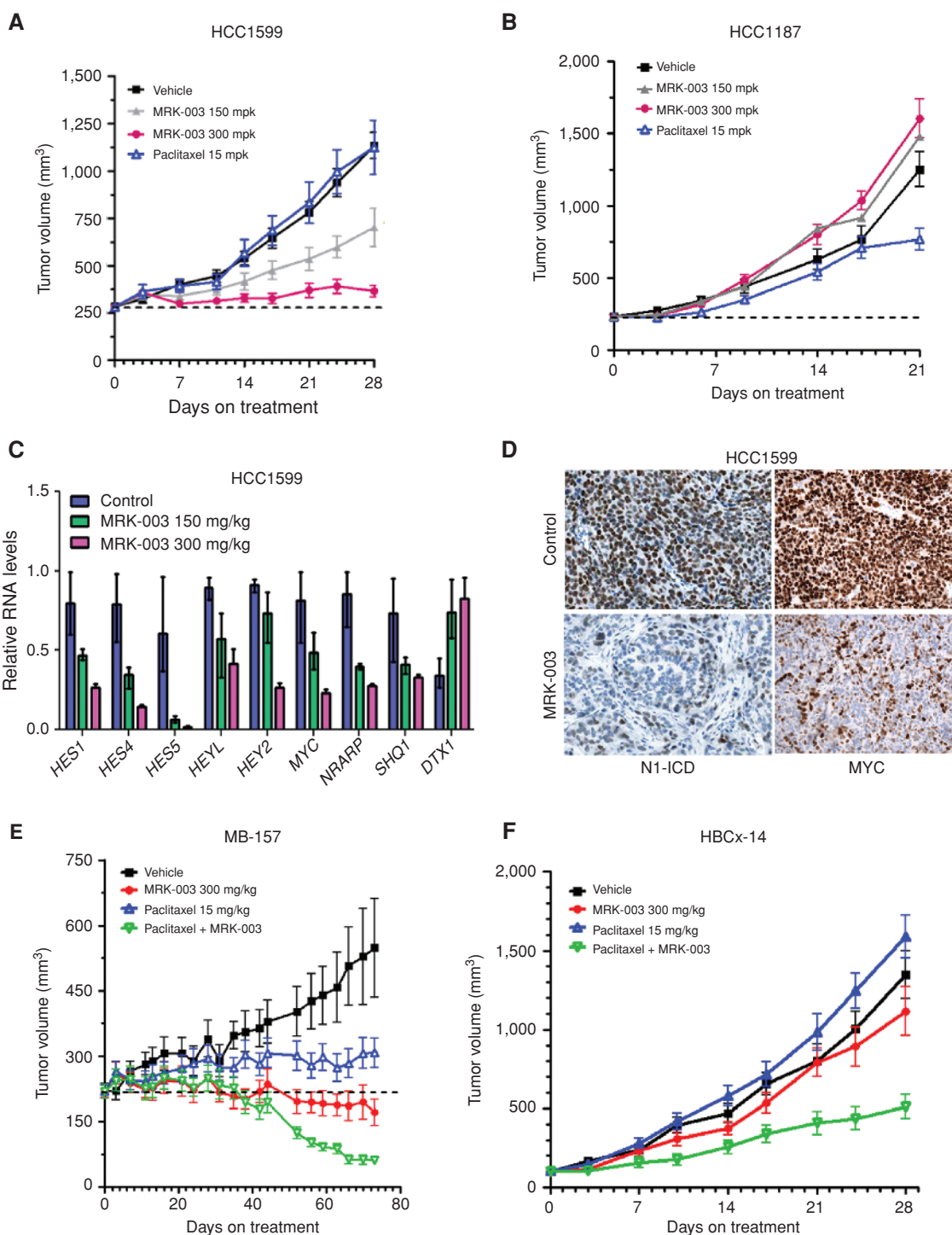


Figure 5. Treatment with MRK-003 leads to tumor regression in NOTCH1-rearranged TNBC xenograft models. **A** and **B**, xenograft models of HCC1599 and HCC1187 cells were treated with 150 or 300 mg/kg MRK-003 once a week, vehicle control, or 15 mg/kg paclitaxel as indicated. A summary of tumor growth inhibition (TGI) is presented in Table 1. MRK-003 treatment at both doses (150 and 300 mg/kg) resulted in significant tumor growth inhibition ($P < 0.001$). **C**, qRT-PCR analysis of tumor tissues from HCC1599 xenografts treated with 150 or 300 mg/kg MRK-003 or vehicle control showing effects of Notch inhibition on a nine-gene signature 6 hours after dosing. HES and HEY family members were significantly downregulated together with MYC, NRARP, and SHQ1, whereas DTX1 (which does not score as a target gene in breast cancer cells) was upregulated. **D**, immunohistochemistry of formalin-fixed paraffin-embedded tumor sections from HCC1599 xenografts treated with 300 mg/kg MRK-003 or vehicle control with an N1-ICD-specific antibody, showing decreased nuclear levels in the MRK-003-treated mice. Tissue was harvested 6 hours after dosing. **E** and **F**, MB-157 and HBCx14 xenograft models, treated with 150 or 300 mg/kg MRK-003 by oral gavage once a week, vehicle control (methylcellulose) or 15 mg/kg paclitaxel, alone or in combination with 300 mg/kg MRK-003. The MB-157 model was treated for 70 days, whereas the HBCx14 model was treated for 28 days. MRK-003 alone or in combination with paclitaxel resulted in significant tumor growth inhibition ($P < 0.001$) in the MB-157 model. In the HBCx14 model, only combination therapy with MRK-003 and paclitaxel was effective ($P < 0.001$).

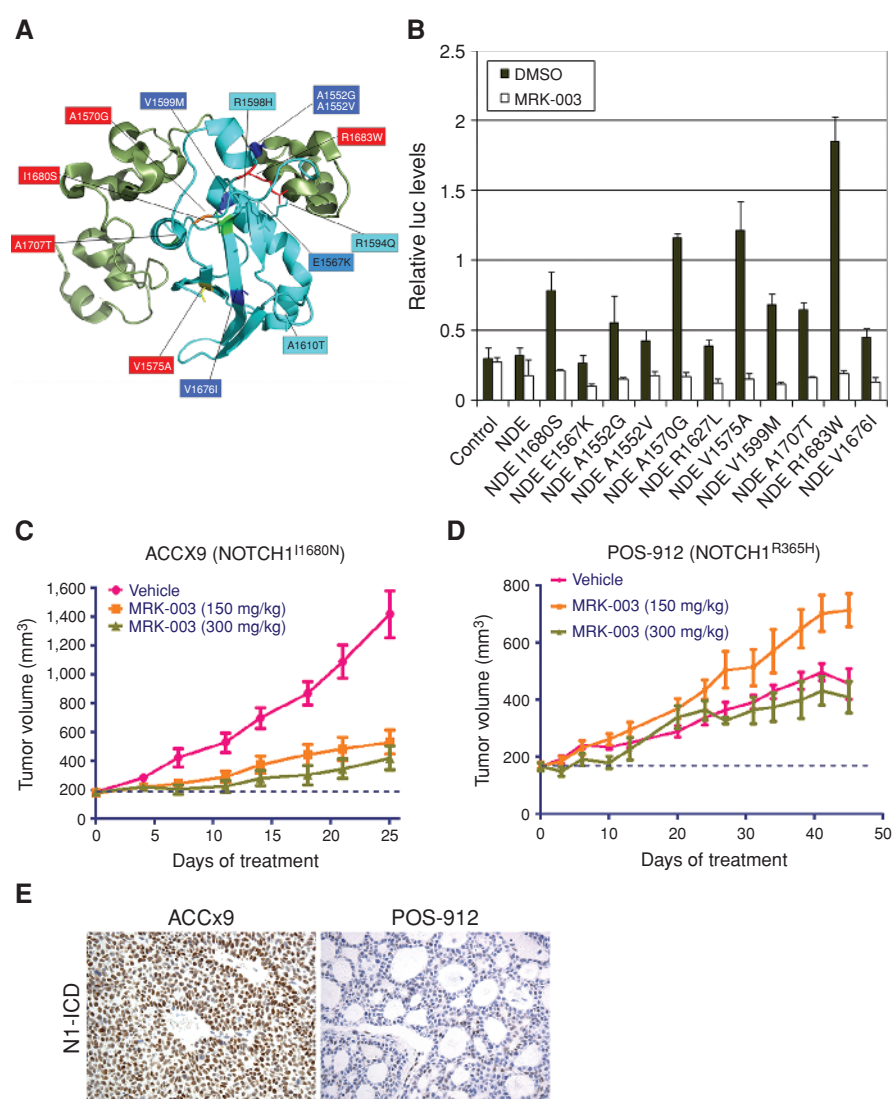


Figure 6. Novel gain-of-function mutations in the NOTCH1 NRR are MRK-003 sensitive in vitro and in vivo. **A**, ribbon diagram of the NOTCH1 NRR showing the position of the newly identified mutations. The NRR is composed of three LNR-A, B, and C modules (green) and a heterodimerization (HD) domain (blue). All identified mutations localized to the HD domain. **B**, HD domain mutations score as gain-of-function mutations in Notch-sensitive reporter gene assays. Mutations were introduced into a cDNA encoding a form of NOTCH1, ΔEGF, that lacks the NOTCH1 ligand-binding domain and cannot respond to ligand, but is sensitive to NRR mutations that trigger ligand-independent signaling. **C** and **D**, response of patient-derived ACC xenograft models to MRK-003. ACCx9, which harbors an activating NOTCH1 I1680N NRR mutation, and POS-912, which harbors a nonactivating mutation in the NOTCH1 EGF repeat region, were treated with 150 or 300 mg/kg MRK-003, as described. MRK-003 treatment resulted in significant tumor growth inhibition in the ACCx9 model ($P < 0.05$). **E**, immunohistochemistry of formalin-fixed paraffin-embedded tumor sections from ACCx9 or POS-912 xenografts with an N1-ICD-specific antibody, showing the presence of nuclear levels in the ACCx9 model.

resulted in significant growth inhibition in the ACCx9 model (Fig. 6C) that harbors an I1680N NOTCH1 NRR substitution, a mutation known to cause ligand-independent NOTCH1 activation (28). In contrast, MRK-003 treatment did not have any antitumor effect on the POS-912 model (Fig. 6D), which harbors a NOTCH1 R365H point substitution in the EGF repeat region that is not expected to produce NOTCH1 gain-of-function. In line with these expectations, high levels of nuclear N1-ICD were observed in tumor cells in the ACCx9 model, whereas in the POS-912 model, only a minor subset of tumor cells had detectable N1-ICD levels (Fig. 6E). We also observed high levels of MYC positivity (>90% of tumor cells)

in the ACCx9 model, whereas the POS-912 model showed much lower levels of MYC expression (see Supplementary Table S6), suggesting that MYC may be a target of Notch in NOTCH-mutated ACC. It should be noted, however, that high MYC expression was also observed in some ACCs with WT NOTCH1 genes, such as the ACCx6 model, suggesting that MYC may sometimes be dysregulated in ACC through mechanisms unrelated to NOTCH1 mutations or NOTCH1 activation. In other analyses, we did not detect an association between NOTCH mutational status and HES4 expression in ACC models (data not shown), emphasizing the need to validate biomarkers of Notch activation in each cellular context

of interest, and suggesting that the most reliable biomarker of Notch activation is direct assessment of NICD levels. Further evaluation of N1-ICD in primary ACC is needed to determine the prevalence of Notch pathway activation in this neoplasm, which appears to be a candidate for treatment with anti-Notch therapies such as GSIs.

DISCUSSION

Aberrant Notch signaling has been implicated in numerous human diseases, including different types of cancers. Through unbiased sequencing of diverse cancer cell lines and primary tumors, we identified different types of activating Notch mutations in specific cancer subtypes. One striking finding is that deletions that remove the coding sequences of NOTCH1 and NOTCH2 ectodomains appear to be highly specific among human tumors for TNBC. It is of interest to note that structurally similar *Notch1* deletions are common in murine T-ALL, where they are caused by DNA breakage at cryptic RAG recombinase sites (4). It is possible that underlying abnormalities of DNA repair make TNBC cells susceptible to activating NOTCH gene deletions caused by random DNA breakage followed by nonhomologous end joining (29). Recent studies by Shah and colleagues (30) observed a high degree of clonal and mutational diversity in TNBC, suggestive of genomic instability. In contrast, in human tumors with relatively small numbers of genetic changes, such as ACC and human T-ALL, Notch gain-of-function mutations tend to consist mainly of point substitutions and small indels.

Several recent tumor genome sequencing studies have identified activating mutations in the Notch signaling pathway in a minority of ACCs (27, 31, 33). Ross and colleagues (33) reported genomic alterations in NOTCH1 in 11% (3 of 28) of ACCs, whereas Ho and colleagues (31) reported alterations in NOTCH signaling pathway genes in 13% of samples. Stephens and colleagues (27) reported activating mutations in NOTCH2 and loss-of-function mutations in SPEN, a gene encoding a transcriptional repressor that forms a complex with RBPJ and downregulates Notch target genes. We did not observe mutations in SPEN in our primary tumor dataset, and it remains to be determined whether SPEN-mutated tumors and NOTCH-mutated tumors are comparable in terms of activation of downstream genes.

It might be anticipated that activating mutations in NOTCH genes would be robust predictors of tumor response to Notch pathway inhibitors such as GSIs, because recurrent mutation of oncogenes in particular types of tumors reliably identifies genes and pathways that are subject to selection during the initiation and progression of cancers. However, although GSIs have been proven safe (34), they are yet to be proven effective, and early experience with human T-ALL suggests that NOTCH gene mutational status, *per se*, is not highly correlated with response. Thus, additional biomarkers that are better predictors of response, preferably across a broad spectrum of cancers that are driven by Notch gain-of-function mutations, are highly desirable.

On the basis of the response of breast cancer and ACC xenografts to MRK-003, it appears that immunohistochemical staining for activated NOTCH1 (N1-ICD) may be one

such biomarker. Xenografts with high levels of N1-ICD immunoreactivity showed excellent responses to GSI, alone and in combination with paclitaxel, whereas xenografts with low N1-ICD reactivity or GSI-refractory rearrangements in NOTCH2 show no response to GSI. It is notable in this regard that NOTCH1 mutations in human T-ALL were discovered through a cell line screen for GSI sensitivity in which the most sensitive cell lines were found to be those with dual NOTCH1 NRR and PEST domain mutations in *cis*, an alignment that produces high levels of N1-ICD (2). Our data suggest that it should be possible to select patients for clinical trials of GSI based on N1-ICD immunoreactivity in archival formalin-fixed paraffin-embedded tissue sections, which would enable rapid screening and identification of patients who are most likely to respond to GSI treatment. Of note, the neoepitopes created by GS cleavage of NOTCH2, NOTCH3, and NOTCH4 are distinct from that created by GS cleavage of NOTCH1, and, in principle, it should be possible to extend this approach to other members of the Notch receptor family, pending development of additional, NICD isoform-specific antibody reagents.

Another biomarker emerging at the interface of expression profiling and genomic analysis is HES4, which is one of a small number of genes that are common to the Notch-driven gene signatures in breast cancer, T-ALL, and B-cell lymphoma cell lines. HES4 expression is also well correlated with NOTCH mutational status in diverse cell lines, and identifies a group of patients with poor prognosis in TNBC. These data suggest that HES4 is a potentially valuable biomarker in certain tumor types such as breast cancer, with the important caveat that the results shown here need to be validated in independent clinical cohorts.

METHODS

Detailed methods for cell growth assays, cell-cycle analysis, stem cell marker analysis, luciferase reporter assays, whole-exome sequencing, exome imbalance analysis, and RNA-seq analysis are provided in Supplementary Methods.

Cell Lines

The T-ALL cell line CUTLL1 (kind gift from Adolfo Ferrando, Columbia University, New York, New York) was cultured in RPMI-1640 containing 10% FBS and 1% penicillin-streptomycin-glutamine. Other cell lines were purchased from cell line banks [ATCC, Japanese Collection of Research Bioresources Cell Bank (RIKEN), or Deutsche Sammlung von Mikroorganismen und Zellkulturen (DKMZ)] and were grown under culture conditions recommended by the vendors. The authenticity of the cell lines was verified by short tandem repeat (STR) profiling analysis or similar methodologies by the banks. In addition, the mutation and gene expression levels from the TES data were compared with the published mutation (Catalogue of Somatic Mutations in Cancer; Sanger database) and gene expression data.

Western Blotting

Cells were lysed in 50 mmol/L Tris, pH 8.0, containing 150 mmol/L NaCl and 1% NP40 supplemented with Protease Inhibitor Cocktail (Thermo Scientific). Protein amounts were determined using the Bio-Rad DCTM Protein Assay Kit II according to the manufacturer's protocol. Samples were mixed with Laemmli sample buffer (Bio-Rad) containing 5% β-mercaptoethanol, separated by 6% or 4% to 15% SDS-PAGE (Bio-Rad), and transferred onto a polyvinylidene

RESEARCH ARTICLE

Stoeck et al.

difluoride (PVDF) membrane using an iBlot dry transfer apparatus (Invitrogen). The membrane was blocked with 5% non fat dry milk (Bio-Rad) or 3% BSA (Sigma) in TBST (20 mmol/L Tris-HCl, 0.5 mol/L NaCl, and 0.1% Tween 20) and incubated with a primary antibody overnight at 4°C. Following washes with TBST, the membrane was incubated with horseradish peroxidase-conjugated secondary antibody (The Jackson Laboratory) and detected with ECL developing solution (Thermo Scientific). A list of primary antibodies used is provided in Supplementary Table S7.

Immunohistochemistry

Standard 5-μm paraffin-embedded tissue sections from xenografts were stained using an anti-N1-ICD rabbit monoclonal antibody (Cell Signaling Technology; clone D3B8, catalog #4147; final concentration, 17 μg/mL), as previously described (19).

GSI Washout Assay

CUTLL1, REC-1, and HCC1599 cells were cultured for 3 days with GSI (compound E; 1 μmol/L) to establish a Notch-off state. Notch was then reactivated by GSI washout as described (22) and harvested for analysis 4 hours later.

Quantitative Real-Time PCR

RNA was extracted from cultured cells or tumor xenografts using the RNeasy Mini Kit (Qiagen). cDNA was synthesized using Super-Script VILO MasterMix (Invitrogen). Quantitative PCR (qPCR) was performed on an ABI 7900 using TaqMan Gene Expression Master-Mix (Invitrogen) and their inventoried TaqMan probes/primers (Supplementary Table S8); the resulting qPCR data were analyzed using the ΔΔC_r relative quantification protocol.

ChIP-qPCR

NOTCH1 and RBPJ ChIP were performed as described (8). REC-1 cells were crosslinked with 1% formaldehyde for 10 minutes at 37°C and sheared by sonication. Rabbit IgG (Jackson ImmunoResearch 011-000-003), NOTCH1 (35), and RBPJ (Cell Signaling Technology; #5313) antibodies were added to the sonicate and incubated overnight at 4°C. DNA-protein complexes were captured with protein A-conjugated agarose beads, washed, and eluted. After reversal of cross-links, DNA was purified using the QIAquick PCR Purification Kit (Qiagen). Input control was prepared in parallel without immunoprecipitation. Real-time PCR was performed in triplicate using primers specific for the *HES4* promoter and genomic negative control. The primer sequences are as follows: *HES4*: forward, 5'-GGTGTGTGAAAC CCGGCTCCG-3'; reverse, 5'-CCGAGGCCTGACTGACAGCG-3'. Genomic negative control primers: forward, 5'-ATGCTGGGCT TCCAAGGA-3'; reverse, 5'-GACCTTGGTGAATGTTGAGAAC-3'.

Xenograft Models

From 1 to 8 × 10⁶ HCC1599, HCC1187, MB157, or MDA-MD-231 TNBC cells were inoculated subcutaneously into the left flank of 4- to 6-week-old immunodeficient (nu/nu or NOD/SCID) female mice (Charles River Laboratories). Patient-derived subcutaneous xenograft efficacy studies included the TNBC models HBCx8 and HBCx14 (Xentech) and the ACC models CTG-0007 (ACCx9) and CTG-0009 (POS-912; Champions Oncology Inc.). Upon reaching an average tumor size of 150 to 250 mm³, mice were randomized across control or treatment groups (*n* = 10–12 mice per group). Tumor size was measured with calipers, and body weight was recorded twice per week during the dosing phase. MRK-003 in 0.5% methylcellulose was given orally at the indicated dose/schedules, whereas paclitaxel in 0.9% NaCl was administered intraperitoneally at a 15 mg/kg once per week. Mice were euthanized at the indicated time points and portions of the tumors were snap-frozen in liquid nitrogen for biochemical

analysis or fixed in 10% neutral buffered formalin for immunohistochemical analysis.

NOTCH Gene Analysis in Human Breast Tumors

Detailed analyses of human tumor cell lines and breast tumors are provided in Supplementary Methods. A summary of the *NOTCH* gene coverage data from human tumors is provided (see Supplementary Table S9; cell line sequencing data can be accessed at Gene Bank accession number SRP044150). *NOTCH* gene signature analysis is provided in Supplementary Table S10.

Disclosure of Potential Conflicts of Interest

C. Ware is Senior Scientist at Merck & Co., Inc. C. Moskaluk is a consultant/advisory board member for Novartis. X.S. Liu is a guest professor at Tongji University. J.C. Aster is a consultant/advisory board member for Cell Signaling Technology and CytomX, Inc. S. Sathyaranarayanan was Principal Scientist at Merck & Co., Inc. No potential conflicts of interest were disclosed by the other authors.

Authors' Contributions

Conception and design: S. Lejnire, L. Zawel, S. Fawell, T. Zhang, W.S. Pear, J.C. Aster, S. Sathyaranarayanan

Development of methodology: S. Lejnire, A. Truong, C. Zang, M. Kluk, B.B. Haines, B.E. Kremer, X.S. Liu, J.C. Aster, S. Sathyaranarayanan

Acquisition of data (provided animals, acquired and managed patients, provided facilities, etc.): A. Stoeck, A. Truong, L. Pan, H. Wang, J. Yuan, C. Ware, P.W. Garrett-Engele, M. Kluk, J. Laskey, C. Moskaluk, B.E. Kremer, B. Knoechel, W.S. Pear

Analysis and interpretation of data (e.g., statistical analysis, biostatistics, computational analysis): A. Stoeck, S. Lejnire, A. Truong, H. Wang, C. Zang, J. Yuan, J. MacLean, M. Kluk, J. Laskey, B.B. Haines, S. Fawell, G. Gilliland, T. Zhang, B.E. Kremer, B.E. Bernstein, X.S. Liu, J.C. Aster, S. Sathyaranarayanan

Writing, review, and/or revision of the manuscript: A. Stoeck, S. Lejnire, C. Zang, J. MacLean, M. Kluk, B.B. Haines, S. Fawell, G. Gilliland, T. Zhang, W.S. Pear, X.S. Liu, J.C. Aster, S. Sathyaranarayanan

Administrative, technical, or material support (i.e., reporting or organizing data, constructing databases): C. Zang, J. Laskey, B. Knoechel

Study supervision: S. Fawell, G. Gilliland, B.E. Bernstein, X.S. Liu, J.C. Aster, S. Sathyaranarayanan

Other (performed immunohistochemistry): C. Ware, M. Kluk

Grant Support

The majority of this work was funded by Merck & Co., Inc. J.C. Aster and W.S. Pear were supported by NIH P01 grant (5P01CA119070-08) and W.S. Pear was supported in part by an Abramson Cancer Center Support Grant from the NCI. B.E. Bernstein acknowledges support from the Adenoid Cystic Carcinoma Research Foundation. B.E. Kremer is supported by NIH K32 Grant CA009615.

Received November 1, 2013; revised July 31, 2014; accepted August 1, 2014; published OnlineFirst August 7, 2014.

REFERENCES

1. Kopan R. Notch signaling. *Cold Spring Harb Perspect Biol* 2012;4:pii: a011213.
2. Weng AP, Ferrando AA, Lee W, Morris JP, Silverman LB, Sanchez-Irizarry C, et al. Activating mutations of NOTCH1 in human T cell acute lymphoblastic leukemia. *Science* 2004;306:269–71.
3. Ellisen LW, Bird J, West DC, Soreng AL, Reynolds TC, Smith SD, et al. TAN-1, the human homolog of the *Drosophila* notch gene, is broken by chromosomal translocations in T lymphoblastic neoplasms. *Cell* 1991;66:649–61.

4. Ashworth TD, Pear WS, Chiang MY, Blacklow SC, Mastio J, Xu L, et al. Deletion-based mechanisms of Notch1 activation in T-ALL: key roles for RAG recombinase and a conserved internal translational start site in Notch1. *Blood* 2010;116:5455–64.
5. Robinson DR, Kalyana-Sundaram S, Wu YM, Shankar S, Cao X, Ateeq B, et al. Functionally recurrent rearrangements of the MAST kinase and Notch gene families in breast cancer. *Nat Med* 2011;17:1646–51.
6. Stransky N, Egloff AM, Tward AD, Kostic AD, Cibulskis K, Sivachenko A, et al. The mutational landscape of head and neck squamous cell carcinoma. *Science* 2011;333:1157–60.
7. Agrawal N, Frederick MJ, Pickering CR, Bettegowda C, Chang K, Li RJ, et al. Exome sequencing of head and neck squamous cell carcinoma reveals inactivating mutations in NOTCH1. *Science* 2011;333:1154–7.
8. Wang NJ, Sanborn Z, Arnett KL, Bayston LJ, Liao W, Proby CM, et al. Loss-of-function mutations in Notch receptors in cutaneous and lung squamous cell carcinoma. *Proc Natl Acad Sci U S A* 2011;108:17761–6.
9. Aster JC, Blacklow SC. Targeting the notch pathway: twists and turns on the road to rational therapeutics. *J Clin Oncol* 2012;30:2418–20.
10. Lehmann BD, Bauer JA, Chen X, Sanders ME, Chakravarthy AB, Shyr Y, et al. Identification of human triple-negative breast cancer subtypes and preclinical models for selection of targeted therapies. *J Clin Invest* 2011;121:2750–67.
11. Lewis HD, Leveridge M, Strack PR, Haldon CD, O'Neil J, Kim H, et al. Apoptosis in T cell acute lymphoblastic leukemia cells after cell cycle arrest induced by pharmacological inhibition of notch signaling. *Chem Biol* 2007;14:209–19.
12. Palomero T, Barnes KC, Real PJ, Glade Bender JL, Sulis ML, Murty VV, et al. CUTLL1, a novel human T-cell lymphoma cell line with t(7;9) rearrangement, aberrant NOTCH1 activation and high sensitivity to gamma-secretase inhibitors. *Leukemia* 2006;20:1279–87.
13. Wang H, Zang C, Taing L, Arnett KL, Wong YJ, Pear WS, et al. NOTCH1-RBPJ complexes drive target gene expression through dynamic interactions with superenhancers. *Proc Natl Acad Sci U S A* 2014;111:705–10.
14. Morris EJ, Jha S, Restaino CR, Dayananth P, Zhu H, Cooper A, et al. Discovery of a novel ERK inhibitor with activity in models of acquired resistance to BRAF and MEK inhibitors. *Cancer Discov* 2013;3:742–50.
15. Palomero T, Sulis ML, Cortina M, Real PJ, Barnes K, Ciofani M, et al. Mutational loss of PTEN induces resistance to NOTCH1 inhibition in T-cell leukemia. *Nat Med* 2007;13:1203–10.
16. Wu CH, van Riggelen J, Yetil A, Fan AC, Bachireddy P, Felsher DW. Cellular senescence is an important mechanism of tumor regression upon c-Myc inactivation. *Proc Natl Acad Sci U S A* 2007;104:13028–33.
17. McGowan PM, Simedrea C, Ribot EJ, Foster PJ, Palmieri D, Steeg PS, et al. Notch1 inhibition alters the CD44hi/CD24lo population and reduces the formation of brain metastases from breast cancer. *Mol Cancer Res* 2011;9:834–44.
18. Mazzone M, Selfors LM, Albeck J, Overholtzer M, Sale S, Carroll DL, et al. Dose-dependent induction of distinct phenotypic responses to notch pathway activation in mammary epithelial cells. *Proc Natl Acad Sci U S A* 2010;107:5012–7.
19. Kluk MJ, Ashworth T, Wang H, Knoechel B, Mason EF, Morgan EA, et al. Gauging NOTCH1 activation in cancer using immunohistochemistry. *PLoS ONE* 2013;8:e67306.
20. Clementz AG, Rogowski A, Pandya K, Miele L, Osipo C. NOTCH-1 and NOTCH-4 are novel gene targets of PEA3 in breast cancer: novel therapeutic implications. *Breast Cancer Res* 2011;13:R63.
21. Rao SS, O'Neil J, Liberator CD, Hardwick JS, Dai X, Zhang T, et al. Inhibition of NOTCH signaling by gamma secretase inhibitor engages the RB pathway and elicits cell cycle exit in T-cell acute lymphoblastic leukemia cells. *Cancer Res* 2009;69:3060–8.
22. Weng AP, Millholland JM, Yashiro-Ohtani Y, Arcangeli ML, Lau A, Wai C, et al. c-Myc is an important direct target of Notch1 in T-cell acute lymphoblastic leukemia/lymphoma. *Genes Dev* 2006;20:2096–109.
23. Palomero T, Lim WK, Odom DT, Sulis ML, Real PJ, Margolin A, et al. NOTCH1 directly regulates c-MYC and activates a feed-forward-loop transcriptional network promoting leukemic cell growth. *Proc Natl Acad Sci U S A* 2006;103:18261–6.
24. Sharma VM, Calvo JA, Draheim KM, Cunningham LA, Hermance N, Beverly L, et al. Notch1 contributes to mouse T-cell leukemia by directly inducing the expression of c-myc. *Mol Cell Biol* 2006;26:8022–31.
25. Klinakis A, Szabolcs M, Politis K, Kiaris H, Artavanis-Tsakonas S, Efstratiadis A. Myc is a Notch1 transcriptional target and a requisite for Notch1-induced mammary tumorigenesis in mice. *Proc Natl Acad Sci U S A* 2006;103:9262–7.
26. South AP, Cho RJ, Aster JC. The double-edged sword of Notch signaling in cancer. *Semin Cell Dev Biol* 2012;23:458–64.
27. Stephens PJ, Davies HR, Mitani Y, Van Loo P, Shlien A, Tarpey PS, et al. Whole exome sequencing of adenoid cystic carcinoma. *J Clin Invest* 2013;123:2965–8.
28. Sanchez-Irizarry C, Carpenter AC, Weng AP, Pear WS, Aster JC, Blacklow SC. Notch subunit heterodimerization and prevention of ligand-independent proteolytic activation depend, respectively, on a novel domain and the LNR repeats. *Mol Cell Biol* 2004;24:9265–73.
29. Amir E, Seruga B, Serrano R, Ocana A. Targeting DNA repair in breast cancer: a clinical and translational update. *Cancer Treat Rev* 2010;36:557–65.
30. Shah SP, Roth A, Goya R, Oloumi A, Ha G, Zhao Y, et al. The clonal and mutational evolution spectrum of primary triple-negative breast cancers. *Nature* 2012;486:395–9.
31. Ho AS, Kannan K, Roy DM, Morris LG, Ganly I, Katai N, et al. The mutational landscape of adenoid cystic carcinoma. *Nat Genet* 2013;45:791–8.
32. Frierson HF Jr, Moskaluk CA. Mutation signature of adenoid cystic carcinoma: evidence for transcriptional and epigenetic reprogramming. *J Clin Invest* 2013;123:2783–5.
33. Ross JS, Wang K, Rand JV, Sheehan CE, Jennings TA, Al-Rohil RN, et al. Comprehensive genomic profiling of relapsed and metastatic adenoid cystic carcinomas by next-generation sequencing reveals potential new routes to targeted therapies. *Am J Surg Pathol* 2014;38:235–8.
34. Krop I, Demuth T, Guthrie T, Wen PY, Mason WP, Chinnaiyan P, et al. Phase I pharmacologic and pharmacodynamic study of the gamma secretase (Notch) inhibitor MK-0752 in adult patients with advanced solid tumors. *J Clin Oncol* 2012;30:2307–13.
35. Wang H, Zou J, Zhao B, Johannsen E, Ashworth T, Wong H, et al. Genome-wide analysis reveals conserved and divergent features of Notch1/RBPJ binding in human and murine T-lymphoblastic leukemia cells. *Proc Natl Acad Sci U S A* 2011;108:14908–13.